Available online at www.sciencedirect.com
SCIENCE DIRECT®
PERGAMON
Polyhedron 22 (2003) 3051–3057
POLYHEDRON
www.elsevier.com/locate/poly

$[Cu(4\text{-oxopyrimidinate})_2 \cdot nH_2O]_\infty$: a robust sodalite type metal-organic framework exhibiting a rich host–guest chemistry

Elisa Barea [a], Jorge A.R. Navarro [a,*], Juan M. Salas [a,*], Norberto Masciocchi [b,c,*,1], Simona Galli [b,c], Angelo Sironi [c]

[a] Departamento de Química Inorgánica, Universidad de Granada, Av. Fuentenueva S/N, E-18071 Granada, Spain
[b] Dipartimento di Scienze Chimiche Fisiche e Matematiche, Università dell'Insubria, via Valleggio 11, I-22100 Como, Italy
[c] Dipartimento di Chimica Strutturale e Inorganica, Università di Milano, via G.Venezian 21, I-20133 Milan, Italy

Received 10 April 2002; accepted 5 August 2002

Abstract

Reaction of Cu^{2+} salts with 4-hydroxypyrimidine (4-Hpymo) in water:ammonia (9:1) solutions at room temperature leads to formation of either $[Cu(4\text{-pymo})_2(NH_3)_2(H_2O)_2]$ (**1**) or $[Cu(4\text{-pymo})_2 \cdot nH_2O]_\infty$ (**2**), depending on which crystal nucleation process occurs. Selective formation of **2** is possible by using non-coordinating Et_3N as a base. X-ray diffraction analyses have been performed in both cases showing that **1** is a mononuclear compound in which the heterocyclic ligands monodentately coordinate the copper ions through the N1 nitrogen atom. **2** is a 3D sodalite type open framework, in which each 4-pymo ligand bridges two copper ions through both nitrogen atoms in the N,N'-exobidentate mode. Heating **1** at 110 °C in air generates an amorphous phase (**2a**), which shows the same chemical analysis and spectroscopic properties as dehydrated **2**. Crystalline $[Cu(4\text{-pymo})_2 \cdot nH_2O]_\infty$ (**2**), possesses interesting physico-chemical properties related to its porous nature. Indeed, this material reversibly absorbs N_2 and water vapour with minimal structural changes.

Keywords: 4-Hydroxypyrimidine; Nanoporous material; N,N'-exobidentate mode; Crystal sponge

1. Introduction

The recent application of coordination chemistry to produce porous materials appears to be of high success. Functional materials developed in this way possess high potential for practical applications such as ion exchange, gas storage, heterogeneous catalysis and chemical sensing [1–3]. Deliberate synthesis of a particular 3D structure by means of a self-assembly process is however very difficult [4]. This fact can be attributed to the lack of control over the coordination modes of the metal ions during assembly of extended structures. Thus, subtle changes in organic ligands, reaction conditions or presence of templating agents can be responsible for dramatic structural changes [5]. For example, when reacted with transition metal ions, simple heterocycles can generate a wide diversity of structural motifs ranging from molecular rings, 1D chains or 2D and 3D metal coordination polymers. Pyrazoles and imidazoles have been recently shown to afford, depending on the synthetic strategy used, a variety of very different structural types [6]. Pyrimidines are not an exception and have been successfully applied for generating both finite and infinite polygonal assemblies with a rich functional and structural diversity [7–10]. We have recently started to study the interaction of transition metal fragments with the symmetric 2-hydroxypyrimidine ligand (2-Hpymo) and found that self-assembly processes lead to discrete cyclic structures [11,12], 1D linear [13] or helical [14] polymers, 2D and 3D coordination polymers [15,16] in which 2-pymo bridges two metal ions through both nitrogen atoms in the N,N'-exobidentate mode. Of special interest is the 3D polymer $[Cu(2\text{-pymo})_2]_\infty$ which

* Corresponding authors. Tel.: +34-958240442; fax: +34-958248526.
E-mail addresses: jarn@ugr.es (J.A.R. Navarro), norberto.masciocchi@uninsubria.it (N. Masciocchi).
[1] Fax: +39-0312386119.

0277-5387/$ - see front matter © 2003 Elsevier Ltd. All rights reserved.
doi:10.1016/j.poly.2002.08.001

possesses a sodalite type open framework that reversibly encapsulates a number of guest molecules within its channels and voids [16]. Moreover, this framework possesses a certain plasticity upon encapsulation of certain inorganic salts, behaving as a so-called third generation material [17]. On attempting parallel syntheses with 4-Hpymo, of lower symmetry than 2-Hpymo, we have observed the formation of either a monomeric compound of formula $[Cu(4\text{-pymo})_2(NH_3)_2(H_2O)_2]$ (**1**) or the polymer $[Cu(4\text{-pymo})_2 \cdot nH_2O]_\infty$ (**2**) which possesses a 3D sodalite type open framework, analogous to previously reported $[Cu(2\text{-pymo})_2]_\infty$, but different affinity for guests molecules as a result of the different stereochemistry of pores.

2. Experimental

2.1. General methods

4-Hydroxypyrimidine (4-Hpymo, Aldrich Chemical Co.) was used as received. The other chemical reagents and solvents were purchased from available commercial sources and used as received. *Caution!* Perchlorate salts are potentially explosive and should be used in small quantities. Magnetic susceptibility measurements were performed on polycrystalline samples with a Quantum Design MPMS-2SQUID magnetometer operating in the range 2.0–300 K at 10 000 G. Powder X-ray diffractograms were performed on Philips PW1000 and PW1820 diffractometers using Cu Kα radiation ($\lambda = 1.5418$ Å). N_2 adsorption was measured at 77 K on a Gemini 2360 apparatus. Thermogravimetric analyses have been performed on a Shimadzu TGA-50H instrument using a reactive air atmosphere and a heating rate of 20 °C min^{-1}.

2.2. Preparation of $Cu(4\text{-pymo})_2(NH_3)_2(H_2O)_2$ (1) and $Cu(4\text{-pymo})_2 \cdot nH_2O$ (2)

$Cu(ClO_4)_2 \cdot 6H_2O$ (1 mmol) and 4-Hpymo (2 mmol) were dissolved in an aqueous ammonia solution (H_2O:NH_3 9:1, 30 ml). Slow evaporation at room temperature of the resulting deep blue solution gave *alternatively*, within 2 days, plate like blue crystals of **1** or dark purple rhombododecahedral crystals of **2** in 50–60% yield. Both batches are obtained as *pure polycrystalline* samples, which may suggest that crystal nucleation should be the dominant step. Selective formation of **2** with increased yields (95%) is possible by using non-coordinating Et_3N (2 mmol) instead of ammonia. Elemental Anal. Found for **1**: C, 29.8; H, 5.5; N, 24.8%. $C_8H_{16}N_6O_4Cu$ requires C, 29.68; H, 4.98; N, 25.95%. IR (cm^{-1}): 3440 s; 3300 m; 3215 s; 1605 vs; 1540 vs; 1485 s; 1435 vs; 1365 s; 1340 s; 1265 s; 1060 m; 1015 s; 840 s. UV–Vis: 17 200 cm^{-1}. Elemental Anal. Found for **2**: C, 30.7; H, 3.9; N, 17.9%. $C_8H_{12}N_4O_5Cu$ requires C, 31.22; H, 3.93; N, 18.21%. IR (cm^{-1}): 3400 br, s; 1635 vs; 1575 s; 1495 s; 1435 s; 1375 m; 1340 s; 1170 m; 1040 s; 845 s. UV–Vis: 17 200; 28 000 cm^{-1}.

2.3. Conversion of $Cu(4\text{-pymo})_2(NH_3)_2(H_2O)_2$ (1) to $Cu(4\text{-pymo})_2 \cdot 0.5H_2O$ (2a)

Thermal treatment of **1** at 110 °C during 4 h results in a dramatic colour change from deep blue to light blue-green *amorphous* powders, **2a**. Elemental Anal. Found for **2a**: C, 36.7; H, 2.6; N, 21.6%. $C_8H_7N_4O_{2.5}Cu$ requires C, 36.58; H, 2.69; N, 21.33%. IR (cm^{-1}): 3400 br; 1625 vs; 1525 s; 1485 s; 1430 s; 1370 m; 1335 s; 1170 m; 1040 s; 845 s. UV–Vis: 14 000; 28 000 cm^{-1}.

2.4. X-ray crystallography

Single crystal data for compounds **1** and **2** were collected on a Stoe STADI4 system at 293 K using Mo Kα radiation with $\lambda = 0.71069$ Å and absorption corrected by empirical methods. **1** at 293(2) K: $C_8H_{16}N_6O_4Cu$, M = 323.81, blue plates, $0.40 \times 0.20 \times 0.15$ mm, monoclinic, space group $P2_1/c$, $a = 7.189(1)$, $b = 13.833(2)$, $c = 6.954(1)$ Å, $\beta = 116.225(9)°$, 620.4(2) $Å^3$, $Z = 2$, $\rho_{calc} = 1.73$ g cm^{-3}, $\mu = 1.78$ mm^{-1}, min. (max.) transmission 0.62 (0.73). Two thousand eight hundred and ninety-four reflections measured, 2243 unique, 1840 with $F_0^2 > 4\sigma(F_0^2)$ were used to refine 120 parameters to $R1(wR^2) = 0.029(0.072)$, GOF = 1.072 and highest peak in diff. map = 0.42 e $Å^{-3}$. **2** at 293(2) K: $C_8H_{12}N_4O_5Cu$, $M = 307.76$, purple rhombododecahedra, $0.15 \times 0.15 \times 0.15$ mm, cubic, space group $Pn\text{-}3m$, $a = 15.7540(4)$ Å, $V = 3910.0(1)$ $Å^3$, $Z = 12$, $\rho_{calc} = 1.66$ g cm^{-3}, $\mu = 1.70$ mm^{-1}, min. (max.) transmission 0.23 (0.27). Five thousand five hundred and twenty-four reflections measured, 888 unique, 224 with $F_0^2 > 4\sigma(F_0^2)$ were used to refine 66 parameters to $R1(wR^2) = 0.16(0.53)$, GOF = 1.571 and highest peak in diff. map = 0.33 e $Å^{-3}$. Structure solution was found in both cases by means of direct methods and refined on F^2 with SHELX-97 [18]. All non-hydrogen atoms were refined anisotropically with exception of oxygens of crystallisation water molecules located in the voids of $[Cu(4\text{-pymo})_2]_\infty$ framework, which were refined with fixed B_{iso} and free occupancy factors. The final model agrees with a $[Cu(4\text{-pymo})_2 \cdot 3H_2O]_\infty$ formulation, which is coherent with the chemical analysis reported above. Assignment of the atomic species for the ammonia/water ligands in **1** was based upon the observed geometrical features and H atoms location. We have found in **2** a significant disorder in either crystallisation water molecules and pyrimidine moieties, part of which depends on the high space group symmetry of the crystals. Such disorder could be removed neither by lowering the space group symmetry, nor by using fractional occupancies for a number of clathrated water

molecules and the exocyclic pyrimidine O(4) atom. In all cases, the final agreement factors were rather high. Aiming to improve the quality of the structure determination of the beautifully shaped crystals of **2**, we performed a number of additional diffraction experiments, which included partial data collections on: (i) different single crystals, down to −100 °C; (ii) single crystals 'evacuated' by mild thermal treatment (see below) and (iii) powders of monophasic samples of **2**, with and without heating prior to data collection. All these experiments confirmed the proposed structure and the rather unusual *very rapid* decay of the scattered intensity at medium angles (resulting in loss of resolution and very high *apparent* thermal parameters), no matter which dataset was employed. *That systematic errors in these experimental measurements are not prevailing is easily demonstrated by the reproducibility of these effects upon using different sources, geometries, environments and techniques.* Moreover, our powder diffraction data demonstrate that the 3D 'rigid' framework $[Cu(4\text{-pymo})_2]_\infty$ is somewhat flexible, since it can accommodate a varying number of water molecules by simple *isotropic* shrinkage, or expansion, of the cubic lattice. Consequently, we attribute the poor agreement factors obtained by our model not only to the asymmetry of the 4-pymo moieties (possibly with concomitant multiple arrangements of ligands around the copper centres and presence of static disorder, witnessed by an average B_{iso} value of ca. 20 Å^2), but mainly to the presence of the large voids (see later) in which 'liquid-like' water molecule clusters can freely move, or, at low temperature, be freezed in random orientations. Removing the high symmetry constraints of the Cu atom location slightly lowers the agreement factors, at the expenses of a higher number of parameters.

3. Results and discussion

Evaporation of an aqueous ammonia solution containing $Cu(ClO_4)_2 \cdot 6H_2O$ (1 mmol) and 4-Hpymo (2 mmol) randomly yielded mononuclear $[Cu(4\text{-pymo})_2(NH_3)_2\ (H_2O)_2]$ (**1**) or polynuclear $[Cu(4\text{-pymo})_2 \cdot nH_2O]_\infty$ (**2**). We attribute this behaviour to be related to the crystal nucleation process, possibly favoured by the low energetic differences between the thermodynamic processes involved in formation of **1** and **2**. Selective formation of **2** is possible by using non-coordinating Et_3N as base instead of ammonia yielding **2** in the form of a pure microcrystalline product.

Conversion of **1** by thermal dehydration (110 °C, 4 h) leads to an amorphous product with an analytical formula of the $Cu(4\text{-pymo})_2(H_2O)_{0.5}$ type (**2a**). Spectroscopic data (IR, UV–Vis) and other techniques (TGA), as discussed below, coherently suggest that **2a** is a heavily disordered partially dehydrated phase of **2**.

3.1. Crystal structures

A view of the molecular structure of **1** together with its numbering scheme is shown in Fig. 1. A selection of structural parameters for **1** and **2** is listed in Table 1.

Crystals of **1** contain mononuclear $Cu(4\text{-pymo})_2(NH_3)_2(H_2O)_2$ complexes, lying on crystallographic inversion centres. The heterocyclic ring acts here as a conventional monodentate ligand through its N(1) atom, with a refined Cu–N bond distance of 2.020(1) Å. The copper coordination polyhedron is a Jahn–Teller elongated octahedron with the water molecules sitting at the apical positions (2.511(1) Å) and the ammonia (Cu–NH_3 2.018(1) Å) and pyrimidine ligands occupying the equatorial ones in an *all-trans* configuration about the metal centre. The crystal structure is additionally stabilised by an extensive *inter*molecular hydrogen-bonds network between the exocyclic O(4) atom and coordinated ammonia and water molecules of neighbouring molecules (see Fig. 2 and Table 1).

Preliminary X-ray powder diffraction measurements indicated, for **2**, its likely isomorphous nature with the $\{[Cu(2\text{-pymo})_2] \cdot (NH_4ClO_4)_{1/3}\}_\infty$ framework previously reported by us [16]. Indeed, our complex X-ray analysis on single crystals and powders of **2** (see Section 2) confirmed that the combination of 90° and 120° bond angles,

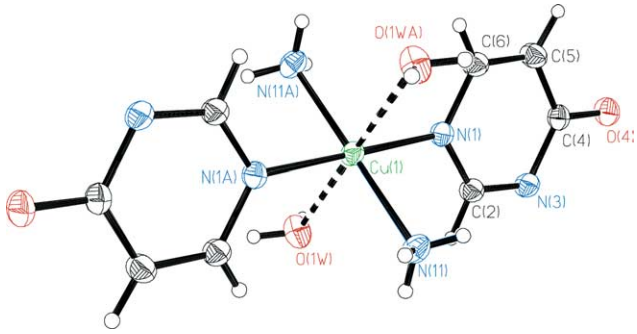

Fig. 1. View of the molecular structure of **1**. Cu is located on a crystallographic inversion center. Ellipsoids are drawn at the 50% probability level.

Table 1
Selected bond distances (Å) and angles (°) and hydrogen-bond distances in the crystal structures of **1** and **2**

	1	**2**
Cu–N(1)	2.020(1)	1.97(2)
Cu–O(1)W	2.511(1)	2.76(3)
Cu–N(11)	2.018(1)	
Cu(1)···Cu(1)		5.5699[i] = $a_0/2\sqrt{2}$
N(1)–Cu–N(1)	180[ii]	94.9(9)[iii]
N(11)···O(4)	2.952(2)[iv]	
N(11)···O(4)	2.963(2)[v]	
O(1)W···O(4)	2.776(2)[vi]	

(i) $1-z, 1-x, 1-y$; (ii) $-x, y+1/2, -z+3/2$; (iii) $x, -y+3/2, -z+1/2$; (iv) $-x, y-1/2, -z+3/2$; (v) $x+1, -y+1/2, z+1/2$; (vi) $x+1, -y+1/2, z+3/2$.

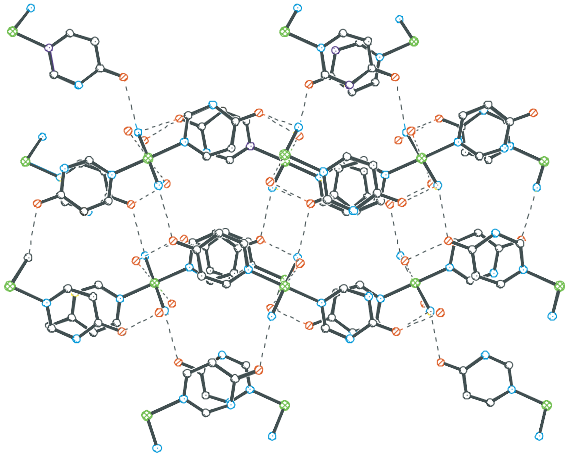

Fig. 2. View, down the crystallographic **c** axis, of the H-bonding interaction scheme in the crystal structure of **1**.

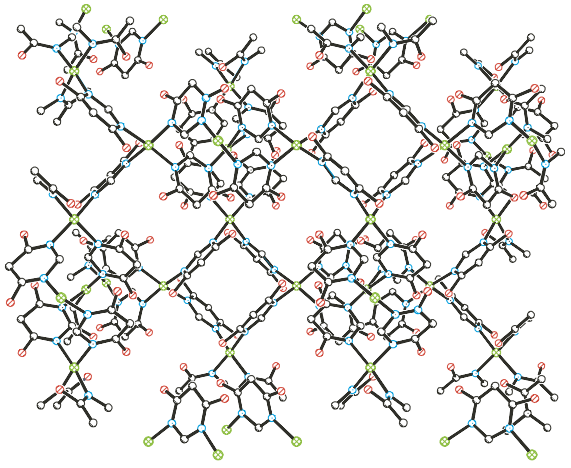

Fig. 3. 3D polymeric $[Cu(4\text{-pymo})_2]_\infty$ framework in crystalline **2**. Water molecules are not included for the sake of clarity.

provided by square-planar copper(II) atoms and pyrimidine-based 'connectors', generates a sodalite type 3D open-framework (see Fig. 3).

A related behaviour has also been recently demonstrated for Cu(imidazolate)$_2$ (blue phase), where Cu–ring centroid–Cu angles are closer to 108° than to 120° [19]. The polymorphic structures reported in [19] and the very existence of **2a** prompt for the possible existence of polymorphism even in the present case, obtainable by slight modifications of the original synthesis. Indeed, for this class of compounds, such 'supramolecular' versatility, in topology and framework dimensionality, is more a rule than an exception [6,19,20]. At variance, the $[M(2\text{-pymo})_2]_\infty$ polymers (M = Co and Zn), with metal ions showing higher propensity than Cu(II) to tetrahedral coordination, have been found to crystallize as diamondoid frameworks [15].

The 3D $[Cu(4\text{-pymo})_2]_\infty$ polymer, which could exist per se, is found to accomodate (at least) two types of water molecules in its porous framework; on the one hand water molecules very loosely coordinated to the metal centres [Cu···O(1)W 2.76(3) Å] and, on the other hand, clathrated water molecules extensively interacting with 'coordinated' ones and the exocyclic oxygen O(4) atoms of the 4-pymo ligands. On the basis of a thorough analysis of the O···O interactions, each copper environment needs likely to be described as an elongated square pyramidal CuN_4O chromophore with a loosely bonded water molecule in the apical position, and, possibly, the metal atom slightly off the 'best' N_4 plane (as indicated by its high thermal parameter, see Section 2). The high symmetry of the crystal system does not permit however unequivocal configuration assignment (Fig. 4), but we presume that when the water molecule is coordinated on one side of the the CuN_4 basal plane, the two exocyclic pyrimidine O(4) atoms *must* be located on the other side, this situation being statistically distrib-

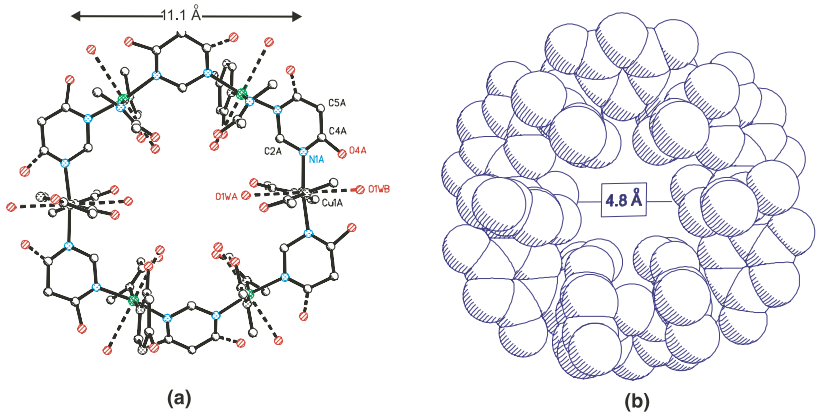

Fig. 4. (a) View of $[Cu(4\text{-pymo})_2]_6$ molecular hexagons that define the closest opening of pores in **2** open framework. Water molecules and exocyclic O(4) have 1/2 occupancy factors due to ambiguous location in the highly symmetric *Pn*-3*m* space group. (b) Space filling representation of the hexagonal pores, taking into account the van der Waals radii.

uted within the crystal bulk. The $[Cu(4\text{-pymo})_2]_\infty$ framework accounts for approximately 80% of the total volume of the crystal, the remaining 20% being associated with pervious pores, typically occupied by water molecules. The closest opening of the pores, taking into account the van der Waals radii, is ~4.8 Å and is defined by the $[Cu_6(4\text{-pymo})_6]$ hexagons shown in Fig. 4.

Large voids of approximate tetrahedral shape are present, each accounting for an approximate 'empty volume' of ~300 $Å^3$, which could, in principle, give molecular sieve properties to crystals of 'evacuated' **2**. With the caveat put forward a few lines ago, *referring to the presence of a conditioned disorder*, we can safely assume that, throughout the crystal, the exocyclic O(4) oxygen atoms are randomly oriented. In other words, we think that the self-assembly process leading to $[Cu(4\text{-pymo})_2]_\infty$ is not accurate enough to direct the formation of a rigorously ordered framework. However, the different shape of the 4-pymo ligand, if compared to 2-pymo, seems to dramatically lower the affinity of **2** toward guest molecules, this effect being discussed in details in the next paragraphs.

3.2. Spectroscopic, magnetic and thermal properties

1 starts to lose weight by dehydration and loss of the ammonia ligands around 90 °C, this process being completed around 200 °C. The resulting material is thermally stable in air up to 270 °C where the pyrolysis process of pyrimidine moieties begins. In the case of **2**, dehydration starts at much lower temperatures (ca. 40 °C) and is complete around 160 °C. Once this process is finished, the decomposition one, following the same path as **1**, finishes around 550 °C to give CuO.

As expected on the basis of the crystals structures described above, the IR spectra of **1** and **2** are significantly different [ν(C=O) 1605 and 1635 cm^{-1}, respectively]. These differences arise both in location and widths of the most diagnostic peaks, which we attribute to the different coordination modes of the pyrimidine ligands [15]. Electronic spectra (diffuse reflectance of the molturated solids) for both compounds show a broad band at 17 000 cm^{-1} due to a d–d transition (with only small differences, i.e., higher intensity for **2** than for **1**); in the case of **2** an additional broad and strong ligand-to-metal charge transfer band appears in the region 32 000 – 23 000 cm^{-1}, which we attribute to the polymeric nature of **2**, where high antiferromagnetic interactions are present (see below) [21]. The IR spectrum of **2a**, obtained by heating **1**, is virtually the same as for **2**, suggesting a change of pyrimidine coordination mode, from *N*-monodentate to *N*,*N*′-exobidentate and concomitant desapparition of the bands at 1265 and 720 cm^{-1} attributed to ammonia ligands. Moreover, also the electronic spectra of dehydrated **2** and **2a** are very similar. The characteristic charge transfer band in the region 32 000 – 23 000 cm^{-1} is present in both materials, in agreement with their polymeric nature. The d–d transition band in **2a**, however, is shifted to lower energies, suggesting a further change in the copper environment, due to enforced dehydration, eventually leading to a distorted tetrahedral CuN_4 chromophore.

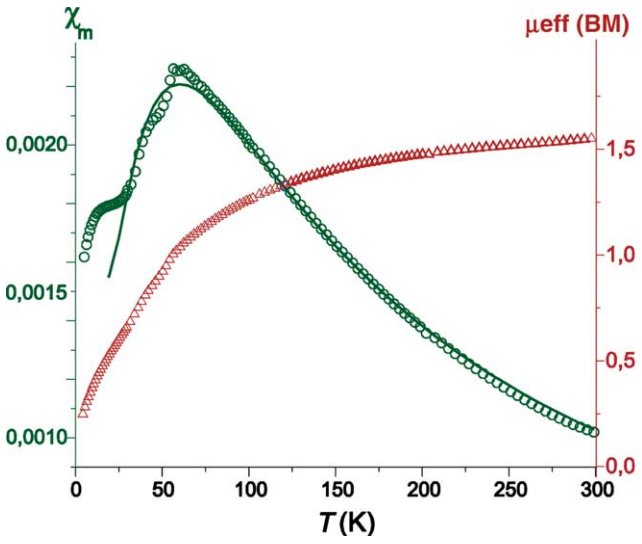

Fig. 5. Temperature dependence of χ (○) and μ_{eff} (△) for **2**. The best fit of χ data using Eq. (1) is shown as a solid line.

The magnetic properties of **2** also agree with its polymeric nature. Indeed, the temperature dependence of the magnetic susceptibility of **2** (see Fig. 5) shows a maximum about 60 K, characteristic of a strong antiferromagnetic exchange between the copper centers. This is also shown by the steady decrease of the μ_{eff} from 1.56 (300 K) to 0.25 BM (2 K). In the 40–300 K temperature range, the magnetic behaviour of **2** can be conveniently described by Eq. (1) that is adequate for description of high temperature dependence of magnetic susceptibility on a 2D Heisenberg quadratic-layer antiferromagnet, [2] where the spin Hamiltonian is defined as $H = \Sigma J,\ S_i \cdot S_j$ [23], $\theta = kT/JS(S+1)$, g is the Landé g factor, μ_B the Bohr magneton and N the number of spins in the lattice. The C_n coefficients have been taken accordingly. [3]

$$\chi = \frac{Ng^2\mu_B^2}{J\left(3\theta + \sum_{n=1}^{\infty}\frac{C_n}{\theta^{n-1}}\right)}, \qquad (1)$$

The best fit parameters are $g = 2.014(3)$ and $J = -44.0(1)$ cm^{-1} for the magnetic data on the 20–300 K range. The agreement factor R defined as $\Sigma(\chi_{M_{cal}} - \chi_{M_{obs}})^2/\Sigma(\chi_{M_{obs}})^2$ is then equal to 2×10^{-9}. This

[2] Although we are aware of the 3D structure of **2** we think this model to be adequate for describing its magnetic behavior since it takes into account the proper connectivity between the paramagnetic metal centres.

[3] For $S = 1/2$, C_n coefficients take the values: $C_1 = 4$; $C_2 = 2.667$; $C_3 = 1.185$; $C_4 = 0.149$; $C_5 = -0.191$; $C_6 = 0.001$.

result agrees with that previously found for the copper/2-hydroxyprimidine polynuclear systems which show analogous magnetic properties [22], confirming that the magnetic interaction can be efficiently transmitted through the pyrimidine bridges. Noteworthy, applying Eq. (1) to magnetic data of $[Cu(2\text{-pymo})_2]_\infty$ [16] gives a slightly lower $J = -36.2(2)$ cm^{-1} exchange value which may be attributed to slightly different electronic nature of the bridge.

3.3. Host–guest properties of 2

We have studied the gas sorption properties of **2**. It has been possible to follow the dehydration–hydration process by diffraction directly on powdered samples as well as on single crystals. The latter, when heated in the 50–140 °C range, maintain their characteristic shape and luster, but shrink to progressively smaller cubic unit cells (down to 15.18 Å), due to water removal. In these conditions, an evacuated $[Cu(4\text{-pymo})_2]_\infty$ framework is obtained, which, differently from what is observed for $[Cu(2\text{-pymo})_2]_\infty$ [16], does not significantly differ from its hydrated congener **2**. A similar observation is also made when the crystals are immersed in dry MeOH which may be accounted for by the removal of the clathrated water molecules. After heating powders of **2** at 140 °C for a few minutes (in air), the colour of the samples shifted from deep to light blue; this obviously means that the Cu(II) chromophore slightly changed, possibly by removal of loose 'axial', Cu···O interactions. On this heated sample, X-ray powder diffraction data were collected at 20 min intervals at 27 °C and 60% relative humidity. The evolution of the cubic lattice parameter from 15.50 to ca. 15.85 Å is depicted in Fig. 6, showing that the asymptotic value is obtained after ca. 7 h. This behaviour is completely reversible and may explain the high thermal factors experienced by these samples, which we attribute to inhomogeneous distribution of water molecules in the pores, with consequent strain of an 'average' unit cell. During the dehydration and rehydration process, the XRPD peaks of Cu(4-pymo)$_2$ maintain their original FWHMs, thus indicating that these processes do not destroy, or significantly modify, the sample crystallinity. In addition, we have found that powder data scans performed on different samples and conditions (within 1 month), showed extreme variability of the lattice parameter, with the upper and lower limits found to lie near 15.96 and 15.20 Å and cell volumes (4065 versus 3511 Å^3) ca. 4% larger (or 10% smaller) that in the single crystal described above. Thus, as demonstrated by our thermal treatment studies, the correct formulation of this class of compounds, *behaving as reversible water sponges*, is $[Cu(4\text{-pymo})_2]\cdot nH_2O$, with n ranging from 0 (evacuated samples) to, possibly, 3 or 4, $n = 3$ being an intermediate formulation of an *average* sample stable at, or near, RT. Summarising, both $[Cu(4\text{-pymo})_2]_\infty$ and $[Cu(2\text{-pymo})_2]_\infty$ frameworks show very high, and comparable, water affinity.

At variance, our results of N_2 sorption experiments, shown in Fig. 7, are surprisingly different for the two porous frameworks, even though that they share similar structural features.

These experiments show a isotherm type I in both cases but N_2 uptake in **2** is depleted to 1/5, if compared to the previously reported $[Cu(2\text{-pymo})_2]_\infty$ material. We attribute this change to the *differently shaped* pores in **2** and $[Cu(2\text{-pymo})_2]_\infty$. Indeed, in $[Cu(2\text{-pymo})_2]_\infty$, six oxygen atoms point to the inner side of the $[Cu_6(2\text{-pymo})_6]$ cavity, while 'hydrophobic' tetrahedral voids contain no oxygen atoms. In **2**, (randomly distributed) exocyclic O(4) atoms point into such tetrahedral cavities, which are now shrinked by their presence and

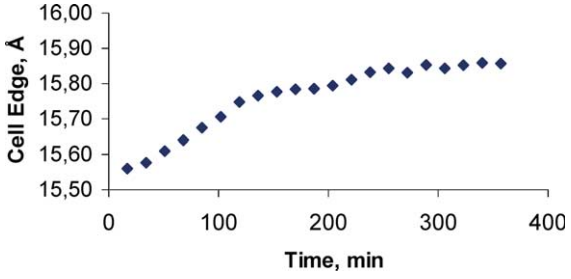

Fig. 6. Time evolution of the cubic lattice parameter a_0 of **2**, upon rehydration at RT.

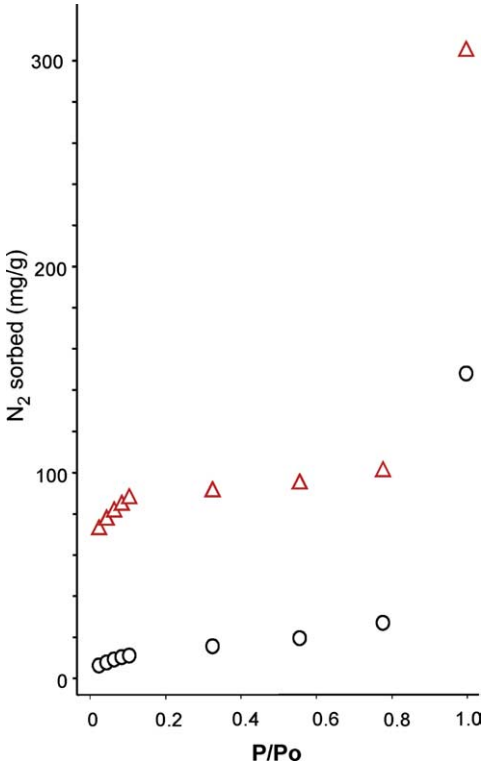

Fig. 7. N_2 sorption isotherm for $[Cu(2\text{-pymo})_2]_\infty$ (△) [16] and **2** (○) at 77 K.

changed into hydrophilic holes. That acid–base effects are a prevailing factor is clearly demonstrated by the depleted affinity of **2** for inorganic salts inclusion. Indeed, we have not observed salt sorption even in lower polarity solvents such as methanol thus less competing than water. Summarising, the $[Cu(2\text{-pymo})_2]_\infty$ salt sorption properties are not present in **2** which may be related to the irregularly shaped pores found in **2**.

4. Conclusions

The formation of the $[Cu(4\text{-pymo})_2]_\infty$ framework is a rare example of a direct synthesis of a 3D coordination material, which can easily occlude water molecules or small ionic systems. The self-assembly process leading to a sodalite-type framework is independent on the position of the substituent oxygen in the pyrimidine ring, the most preferred coordination geometry for such heterocycles being the N,N'-exobidentate mode. However, the actual location of the exocyclic oxygen atom dramatically changes the rich host–guest chemistry of these porous frameworks, through steric, as well as electronic, modifications of the inner surfaces of the active sorption sites. The complex structural analysis of **2**, though incomplete, has taken undoubtful advantages from the coupling of different conventional diffraction experiments (on single crystals and powders), on as-prepared, cooled or heated samples. Such combination of experimental techniques is thought to greatly enhance the comprehension of troublesome specimens, whose relevant crystallochemical features need prolonged efforts in order to be understood. Accordingly, powder diffraction has recently become an unavoidable tool in the material chemist's hands when facing unexpected problems (twinning, metastability, phase-transformation, etc.) even for 'conventional', but often untractable, covalent-molecular or polymeric-species [24].

5. Supplementary material

Crystallographic data (excluding structure factors) for the structures reported in this paper have been deposited with the Cambridge Crystallographic Data Centre supplementary publication No. CCDC-182155 and 182156. Copies of the data can be obtained free of charge on application to CCDC, 12 Union Road, Cambridge CB21EZ, UK (fax: (+44)1223-336-033; e-mail: deposit@ccdc.cam.ac.uk).

Acknowledgements

The Ministerio de Ciencia y Tecnología (Project BQU2001-2955-CO2-01) have supported this research. EB thanks the Ministerio de Educación for a fellowship. The authors are also thankful to Prof. R. Faure (Université Claude Bernard Lyon I) for measuring one of the crystallographic datasets for **2**.

References

[1] M. Eddaoudi, D.B. Moler, H. Li, B.L. Chen, T.M. Reineke, M. O'Keeffe, O.M. Yaghi, Acc. Chem. Res. 34 (2001) 319.
[2] M. Fujita, Y.I. Kwon, S. Washizu, K. Ogura, J. Am. Chem. Soc. 116 (1994) 1152.
[3] J.S. Seo, D. Whang, H. Lee, S.I. Jun, J. Oh, Y.J. Jeon, K. Kim, Nature 404 (2000) 982.
[4] M. Eddaoudi, J. Kim, M. O'Keeffe, O.M. Yaghi, J. Am. Chem. Soc. 124 (2002) 376.
[5] C. Inman, J.M. Knaust, S.W. Keller, Chem. Commun. (2002) 156.
[6] N. Masciocchi, M. Moret, P. Cairati, A. Sironi, G.A. Ardizzoia, G. La Monica, J. Am. Chem. Soc. 116 (1994) 7668.
[7] J.A.R. Navarro, B. Lippert, Coord. Chem. Rev. 222 (2001) 219.
[8] T. Ezuhara, K. Endo, K. Matsuda, Y. Aoyama, J. Am. Chem. Soc. 121 (1999) 3279.
[9] F. Lloret, G. De Munno, M. Julve, J. Cano, R. Ruiz, A. Caneschi, Angew. Chem., Int. Ed. Engl. 37 (1998) 135.
[10] S.W. Keller, Angew. Chem., Int. Ed. Engl. 36 (1997) 247.
[11] (a) J.A.R. Navarro, E. Freisinger, B. Lippert, Inorg. Chem. 39 (2000) 2301;
(b) J.A.R. Navarro, J.M. Salas, Chem. Commun. (2000) 235.
[12] J.A.R. Navarro, E. Freisinger, B. Lippert, Inorg. Chem. 39 (2000) 1059.
[13] M. Quirós, Acta Crystallogr. C 50 (1994) 1236.
[14] N. Masciocchi, G.A. Ardizzoia, G. La Monica, A. Maspero, A. Sironi, Angew. Chem., Int. Ed. Engl. 37 (1998) 3366.
[15] N. Masciocchi, G.A. Ardizzoia, G. LaMonica, A. Maspero, A. Sironi, Eur. J. Inorg. Chem. (2000) 2507.
[16] L.C. Tabares, J.A.R. Navarro, J.M. Salas, J. Am. Chem. Soc. 123 (2001) 383.
[17] (a) S. Kitagawa, M. Kondo, Bull. Chem. Soc. Jpn. 71 (1998) 1739;
(b) R. Kitaura, K. Fujimoto, S. Noro, M. Kondo, S. Kitagawa, Angew. Chem., Int. Ed. 41 (2002) 133.
[18] G.M. Sheldrick, SHELXL97, Program for the Refinement of Crystal Structures, University of Göttingen, Germany, 1997.
[19] N. Masciocchi, S. Bruni, E. Cariati, F. Cariati, S. Galli, A. Sironi, Inorg. Chem. 40 (2001) 5897.
[20] (a) N. Masciocchi, G.A. Ardizzoia, G. La Monica, M. Moret, A. Sironi, Inorg. Chem. 36 (1997) 449;
(b) G.A. Ardizzoia, S. Cenini, G. La Monica, N. Masciocchi, M. Moret, Inorg. Chem. 33 (1994) 1458, and references therein.
[21] (a) J.A.R. Navarro, M.A. Romero, J.M. Salas, M. Quirós, E.R.T. Tiekink, Inorg. Chem. 36 (1997) 4988;
(b) F. Tuczek, E. Solomon, J. Am. Chem. Soc. 116 (1994) 6916.
[22] L.C. Tabares, J.A.R. Navarro, J.M. Salas, M. Willermann, Inorg. Chim. Acta 318 (2001) 166, and references therein.
[23] (a) M.E. Lines, J. Phys. Chem. Solids 31 (1970) 101;
(b) G.S. Rushbrooke, P.J. Wood, Mol. Phys. 1 (1958) 257.
[24] (a) N. Masciocchi, A. Sironi, J. Chem. Soc., Dalton Trans. (1997) 4643;
(b) K.D.M. Harris, M. Tremayne, B.M. Kariuki, Angew. Chem., Int. Ed. 40 (2001) 1626.